Mathematical Modeling Of Bioelectrochemical Wastewater Treatment Using Microbial Fuel Cells

S. Thamizh Suganya, P. Balaganesan, L. Rajendran

Abstract : Mathematical modeling of microbial fuel cell consisting of a bio-catalyzed anode and air cathode is discussed. This model contains a system of non-linear rate equations, whereas non-linear related to bio-electrochemical kinetics and charge transfer. The non-linear differential equation in this model solves using the new approach of the homotopy perturbation method. The concentration of substrate, primary and secondary microbial fuel cell and mediator are obtained in terms of experimental parameters. The effect of various values of the parameters on the concentration is discussed. The analytical solutions are also compared with simulation results and satisfy the agreement is noted.

Keywords : Microbial fuel cell, Mathematical modeling, Non-linear equation, Homotopy Perturbation Method, Cogeneration, Model-based design, Microbial Electrolysis Cell, Dynamic model.

1 INTRODUCTION

Mathematical models played an essential role in developing MFC efficiency and promoting development and process of optimization along with experimental studies [1-3]. In addition, A dynamic model based on MFC ODEs was developed by Pinto et al.[4]. They used a two-population model to describe the anode microbial species, however, and the multiplicative Monod kinetics were used to illustrate the dynamics of biofilm formation. Also regarded the balance for substrates and mediators and used overpotentials of Ohms law and voltage to derive MFC current expression. This model was simply to be implemented and permitted fast numerical simulations. On the basis of anodophilic concentration, open-circuit voltage and internal resistance are determined and it is difficult to experiment with, limiting the applicability of this process. Losses in moving electrons from bacteria to electrode result in potential losses, i.e., losses inactivation, ohmic losses, and concentration losses [5]. Renewable bioenergy waste, with a positive or even negative carbon footprint, is also viewed as one of the ways to mitigate the climate crisis [6, 7].

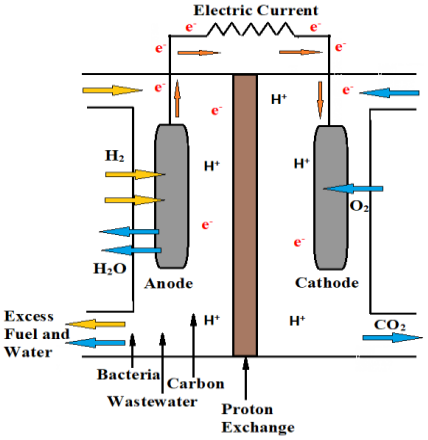

Figure.1 *Microbial Fuel Cell in waste water treatment*

2 MASS BALANCE

The rate of change in substrate and biomass concentrations can be follows [8]:

$$\frac{dS}{dt} = -q_p x_p - q_s x_s \qquad (1)$$

$$\frac{dx_p}{dt} = \mu_p x_p - K_{d_p} x_p \qquad (2)$$

$$\frac{dx_s}{dt} = \mu_s x_s - K_{d_s} x_s \qquad (3)$$

where S is substrate concentration, x is microbial concentration, p and s representsprimary and secondary microbial populations, q is substrate consumption rate, K_d is microbial decay rate and μ is microbial growth rate.

The concentration of oxidized mediator is expressed as follows:

$$\frac{dM_{ox}}{dt} = -Yq_p + \frac{\gamma}{Vx_p}\left(\frac{I_{MFC}}{mF}\right) \qquad (4)$$

The intracellular mediator exists in either oxidized (M_{ox}) or reduced form (M_{red}), however the total mediator concentration M_{total} remains constants. The expression is

$$M_{total} = M_{ox} + M_{red} \qquad (5)$$

The corresponding initial conditions are

$$S = S_{in},\ x_p = x_{pin},\ x_s = x_{\sin},\ M_{ox} = M_{oxin} \quad at \quad t = 0 \qquad (6)$$

where y is dimensionless mediator yield, I_{MFC} is the MFC current, m is the number of electrons transferred per mol of mediator, F is the Faraday constant, V is working volume of the anode chamber, and γ is the molar mass.

$$q_p = q_{max_p}\left(\frac{S}{K_{S_p}+S}\right)\left(\frac{M_{ox}}{K_M+M_{ox}}\right) \qquad (7)$$

$$\mu_p = \mu_{max,p}\left(\frac{S}{K_{S_p}+S}\right)\left(\frac{M_{ox}}{K_M+M_{ox}}\right) \qquad (8)$$

$$q_s = q_{max_s}\left(\frac{S}{K_{S_s}+S}\right) \qquad (9)$$

$$\mu_s = \mu_{max,s}\left(\frac{S}{K_{S_s}+S}\right) \qquad (10)$$

where, K_S Monod half saturation coefficients for substrate and K_M is Monod half saturation mediator, q_{max} and μ_{max} is maximum substrate consumption rate and growth rate.

Equations (7) to (10) substituting in equations (1) to (4) we have the final differential equation as follows

$$\frac{dS}{dt} = -\left(q_{\max p}\left(\frac{1}{K_{S_p}+S}\right)\left(\frac{M_{ox}}{K_M+M_{ox}}\right) + q_{\max s}\left(\frac{x_S}{K_{S_s}+S}\right)\right)S \quad (11)$$

$$\frac{dx_p}{dt} = \left(\mu_{\max,p}\left(\frac{S}{K_{S_p}+S}\right)\left(\frac{M_{ox}}{K_M+M_{ox}}\right) - Kd_p\right)x_p \quad (12)$$

$$\frac{dx_S}{dt} = \left(\mu_{\max,s}\left(\frac{S}{K_{S_s}+S}\right) - Kd_s\right)x_S \quad (13)$$

$$\frac{dM_{ox}}{dt} = -Y\left(q_{\max p}\left(\frac{S}{K_{S_p}+S}\right)\left(\frac{1}{K_M+M_{ox}}\right)\right)M_{ox} + \frac{\gamma}{Vx_p}\frac{I_{MFC}}{mF} \quad (14)$$

3. THE OHM'S LAW AND VOLTAGE LOSSES

The current using Ohm's law as follows [9]:

$$I_{MFC} = \frac{(E_{OCV} - \eta_{conc})}{(R_{ext}+R_{int})}\left(\frac{M_{red}}{\varepsilon + M_{red}}\right) \quad (15)$$

$$E_{OCV} = E_{min} + (E_{max} - E_{min})e^{-\frac{1}{K_{r_1}S}} \quad (16)$$

$$R_{int} = R_{min} + (R_{max} - R_{min})e^{\frac{1}{K_{r_2}S}} \quad (17)$$

$$\eta_{conc} = \frac{RT}{mF}\ln\left(\frac{S_{in}}{S}\right) \quad (18)$$

$$\varepsilon_E = \frac{M_o\int_0^t I_{MFC}dt}{FbV\Delta S} \quad (19)$$

where E_{OCV} is the open circuit voltage, η_{act} and η_{conc} is activation and concentration over potential, R_{ext} and R_{int} are external and internal resistance in the electrochemical cell, E_{min} and E_{max} is lowest and highest observed open circuit voltage, K_{r_1} and K_{r_2} are constants, R is universal gas constant, T is temperature, β is charge transfer coefficient, A_n is surface area, i_0 is exchange current density, ε_E is Coulombic efficiency, M_o is the molecular weight, b is number of electrons exchanged per mol of oxygen, and ΔS is the change in substrate (COD) concentration over time t.

4. ANALYTICAL SOLUTIONS OF THE DIFFERENTIAL EQUATIONS

In this work, the analytical expression of substrate concentration $S(t)$, primary microbial population x_p, secondary microbial population x_s, and oxidized mediator M_{ox} are obtained as follows:

$$S(t) = S_{in}e^{-t\left[\frac{q_{\max p}M_{oxin}x_{pin}}{(K_{S_p}+S_{in})(K_M+M_{oxin})} + \frac{q_{\max s}x_{Sin}}{K_{S_s}+S_{in}}\right]} \quad (20)$$

$$x_p(t) = x_{pin}e^{t\left(\frac{\mu_{\max p}S_{in}M_{oxin}}{(K_{Sp}+S_{in})(K_M+M_{oxin})} - K_{d_p}\right)} \quad (21)$$

$$x_S(t) = x_{Sin}e^{t\left(\frac{\mu_{\max S}S_{in}}{(K_{S_S}+S_{in})} - K_{d_S}\right)} \quad (22)$$

$$M_{ox}(t) = M_{oxin}e^{-t(Yq_p)} + \frac{\gamma E_{OCV}}{Vx_{pin}mFYq_pR_{int}(\varepsilon+M_{red})}\left[M_{total} - M_{total}e^{-t(Yq_p)} - t\frac{YM_{oxin}e^{-t(Yq_p)}}{q_p}\right] \quad (23)$$

where $q_p = q_{\max p}\frac{S_{in}}{(K_{S_p}+S_{in})(K_M+M_{oxin})}$

$$E_{OCV} = E_{\min} + (E_{\max} - E_{\min})e^{-\frac{1}{K_{r_1}S_{in}}}$$

$$R_{\text{int}} = R_{\min} + (R_{\max} - R_{\min})e^{\frac{1}{K_{r_2}S_{in}}}$$

5 NUMERICAL SIMULATION

The homotopy perturbation method was initially proposed by He et al. [10]. This approach is used to find an approximate linear and nonlinear problem. The way has applied to various boundary value problems [11-13]. The new approach of this method to solve the nonlinear problem has recently introduced, resulting in a simple approximate solution in the zero iteration.

6 RESULTS AND DISCUSSION

Figures 2(a) and 2(b), it can be represented that the degradation of the substrate increases when the K_{S_P} and K_M decrease. As shown in Figures 2(c) and 2(d), variations in the Primary MFC consumption rate and Secondary MFC consumption rate do not lead to many deviations in the biomass concentration compared to the other two parameters. Figure 3(a), it is shown that when the specific substrate Primary MFC consumption growth increases, the biomass concentration reaches its steady-state value in a short time. Figures 3(b) to 3(d), represents the concentration profile is decreasing with increasing various values of the parameters. As a result, its biomass coefficient decreases, and boundary decreases. Figure 4(a) illustrate the behaviour of the MFC concentration for various values of $\mu_{\max_p}$. The numerical results represented the effect of increasing values on Primary MFC consumption growth results in a decreasing velocity. The secondary concentration profiles for different values of the $K_{d_s,}$ and K_{S_s} are displays in the Figures 4(b) and 4(c). It is noticed that an increase in the parameters leads to a decrease in the value of MFC concentration. Figures 5(a) and 5(b) depicts the mediator concentration for different values of K_{S_p} and K_M. The parameters increase the peak value of concentration across the boundary layer tends to increase. Figures 5(c) and 5(d) illustrate the effect of primary MFC consumption rate and dimensionless mediator yield on the mediator concentration profile. It represents the concentration profile is decreasing with increasing values of the parameters. In Figure 6(a) represented the effects of the voltage increases, the current is reducing in varies values of the resistance. Figure 6(b) the concentration of oxidized mediator increased during the short-term closed-circuit period and decreased otherwise. This behavior is understandable as the change in concentration of the intracellular mediator's oxidized form during open circuit operation represents a simultaneous charge within the anodic compartment's electrical genic bacteria (biofilm). From the voltage-current curves, it is clear that the MFC functioned with the chosen standard set of parameters functions in a mass-transfer-limited regime in Figure 6(c). Diffusion constraints are growing by the day as biofilms are becoming thicker. These model outputs are very similar to the character relationships of voltage – current and voltage – power observed in real MFC. The initial COD concentration increases in Figure 6(d), with an increase in

the initial COD concentration, the highest voltage produced in the MFC. While at lower values, this rise is strongly linear, it starts plateauing with further growth. Such an increase in voltage may be due to increased exposure to the substratum by the primary microbial population as the initial COD concentration rises. It results in increased metabolic activity, resulting in most of the electrons that can be passed to the anode, resulting in higher voltage generation. Figure 6(e) shows that the concentration is increasing, the resistance is decreasing, and the cell potential measured across resistances showed marked variation with the function of the organic load in Figure 6(f). At lower applied resistance, cell potential started to decrease. The potential anode controls the biocatalyst's electron-energizing ability, during its metabolism electron transport from the substratum to anode, and subsequently to bioelectricity generation. Figure 7(a) represent the sensitive analysis of the parameters of the concentration of substrate and primary, secondary microbial. From the Figure 7(a), it is inferred that the parameters q_{max_p}, K_M , and t has more impact than the other parameters. Similarly, from the Figure 7(b), it is inferred that the parameters K_{d_p} and t has more impact than the other parameters then finally we have found the Figure 7(c) represents sensitive analysis of parameters K_{d_s} has only the most impact parameters.

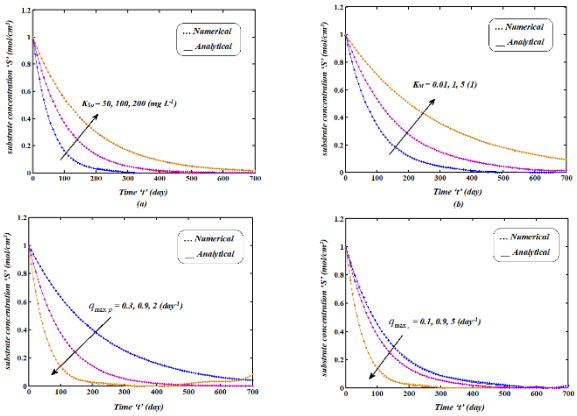

***Figure 2**: substrate concentration of versus time for the various value of the parameter*

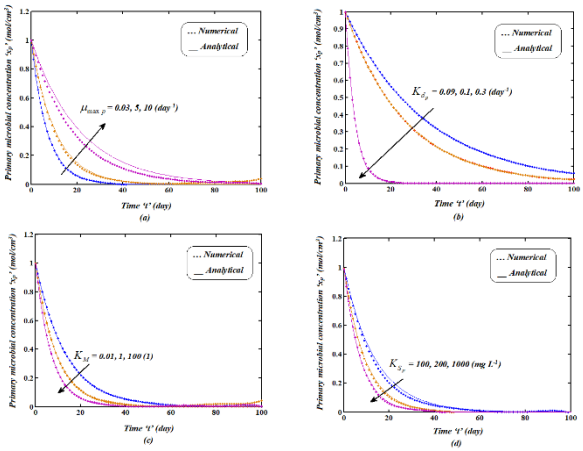

***Figure 3**: Primary microbial concentration of versus time for the various value of the parameter.*

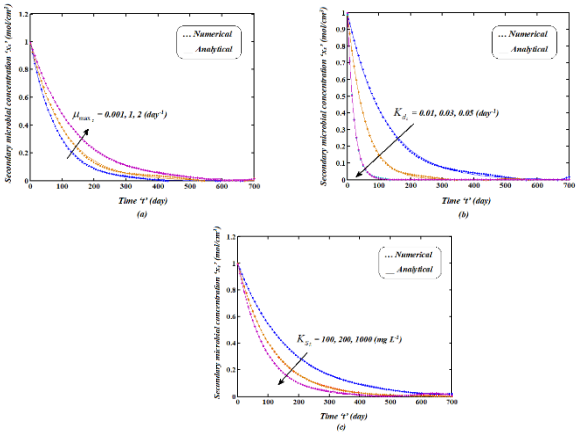

***Figure 4:** Secondary microbial concentration of versus time for the various value of the parameter.*

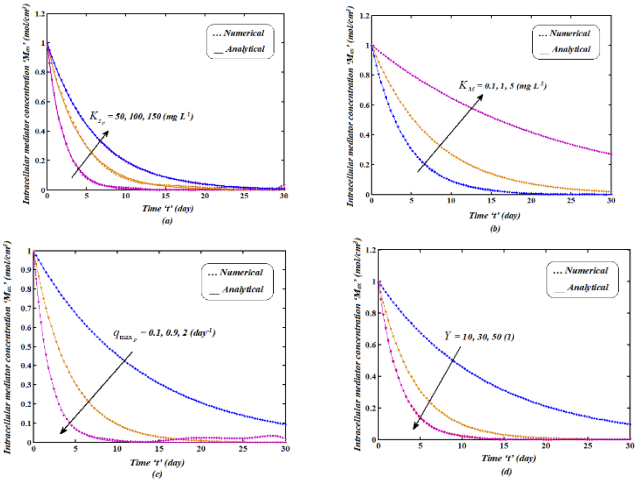

***Figure 5:** Intracellular mediator concentration of versus time for the various value of the parameter.*

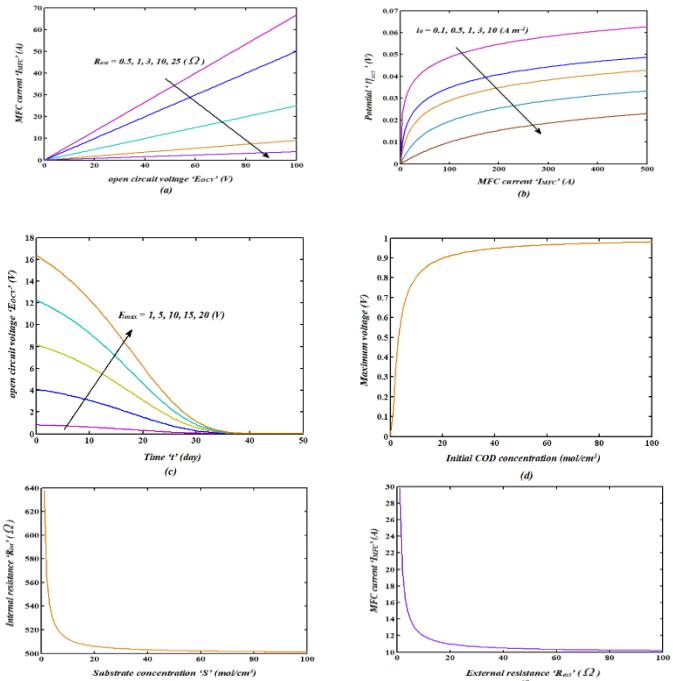

***Figure 6:**Variation of MFC current, Voltage, Current density and Resistance.*

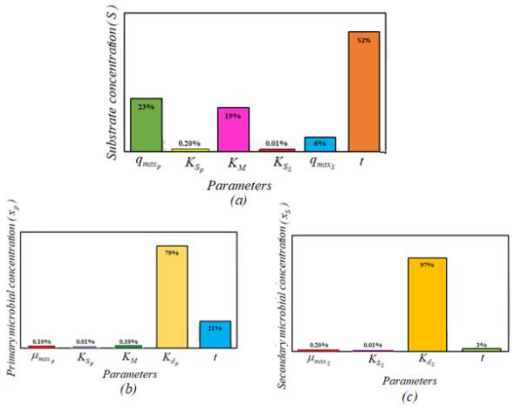

Figure 7: *Sensitive analysis of parameters on substrate concentration MFC concentrations.*

7 CONCLUSION

A non-linear time-dependent system of differential equations in Microbial Fuel Cell has been solved using the new HPM. New approximate analytical expressions for the substrate concentrations, primary and secondary, and secondary microbial concentration, and mediator concentration are derived. The concentration profiles are also presented using the MATLAB program. The obtained results have a good agreement with those obtained using numerical methods.

ACKNOWLEDGMENTS

The authors are also thankful to Shri J. Ramachandran, Chancellor, Col. and Dr.G.Thiruvasagam, Vice-Chancellor, Academy of Maritime Education and Training (AMET), Chennai, Tamil Nadu.

Nomenclature

Parameters	Value	Description and dimension unit
S	-	Substrate concentration (mol/cm^3)
x_p	-	Primary microbial concentration (mol/cm^3)
x_m	-	Secondary microbial concentration (mol/cm^3)
M_{ox}	-	Oxidized mediator concentration (mol/cm^3)
q_{max_p}	0.9	Primary MFC consumption rate (day^{-1})
μ_{max_p}	7.1	Primary MFC consumption growth (day^{-1})
q_{max_s}	0.84	Secondary MFC consumption rate (day^{-1})
μ_{max_s}	0.6	Secondary MFC consumption growth (day^{-1})
K_M	0.11	Monod half saturation coefficients for mediator of one unit
K_{S_s}	425	Monod half saturation coefficients for substrate ($mg\,L^{-1}$)
R_{max}	500	Highest observed internal resistance (Ω)
R_{min}	8	Lowest observed internal resistance (Ω)
i_0	0.048	Exchange current density (A m^{-2})
K_{r_1}	0.5	Slope of the curve ($L\,mg^{-1}$)
K_{r_2}	0.004	Slope of the curve ($L\,mg^{-1}$)
m	2	Number of electrons transferred per mol of mediator of one unit
Y	30.25	Dimensionless mediator yield of one unit
E_{min}	0.01	Lowest observed open circuit voltage (V)
E_{max}	0.66	Highest observed open circuit voltage (V)
K_{d_p}	0.142	Primary microbial decay rate (day^{-1})
K_{d_s}	0.012	Secondary microbial decay rate (day^{-1})
T	298.15	Temperature(K)
γ	663.4	Molar mass ($g\,mol^{-1}$)
K_{S_p}	103	Monod half saturation coefficients for substrate ($mg\,L^{-1}$)
A_n	7	Surface area (cm^2)
V	28	Working volume of the anode chamber (cm^3)
F	96,485	Faraday constant ($As\,mol^{-1}$)
R	8.314	Universal gas constant ($J\,K^{-1}\,mol^{-1}$)
b	4	Number of electrons exchanged per mol of oxygen of one unit
β	0.5	Charge transfer coefficient of one unit
M_0	15.999	Molecular weight (kg mol^{-1})

Appendix - A

Analytical solution of equations (1) to (4) using the HPM method.

Equations (1) to (4) can be written as follows:

$$\frac{dS}{dt} = -\left(q\max_p\left(\frac{1}{KS_p + S}\right)\left(\frac{M_{OX}}{KM + M_{OX}}\right) + q\max_s\left(\frac{x_S}{KS_s + S}\right)\right)S \qquad \text{(A1)}$$

$$\frac{dx_p}{dt} = \left(\mu\max,p\left(\frac{S}{KS_p + S}\right)\left(\frac{M_{OX}}{KM + M_{OX}}\right) - Kd_p\right)x_p \qquad \text{(A2)}$$

$$\frac{dx_S}{dt} = \left(\mu\max,s\left(\frac{S}{KS_s + S}\right) - Kd_s\right)x_S \qquad \text{(A3)}$$

$$\frac{dM_{OX}}{dt} = -Y\left(q\max_p\left(\frac{S}{KS_p + S}\right)\left(\frac{1}{KM + M_{OX}}\right)\right)M_{OX} + \frac{\gamma}{Vx_p}\frac{IMFC}{mF} \qquad \text{(A4)}$$

The initial conditions are

$$S = S_{in},\ x_p = x_{pin},\ x_s = x_{sin},\ M_{ox} = M_{oxin} \quad at \quad t = 0 \qquad \text{(A5)}$$

Homotopy for the above equations (A1) to (A5) can be constructed as follows:

$$(1-p)\left[\frac{dS}{dt}+\left(q_{max_p}\left(\frac{1}{K_{S_p}+S(t=0)}\right)\left(\frac{M_{ox}(t=0)}{K_M+M_{ox}(t=0)}\right)+q_{max_s}\left(\frac{x_s(t=0)}{K_{S_s}+S(t=0)}\right)\right)S\right]$$
$$+p\left[\frac{dS}{dt}+\left(q_{max_p}\left(\frac{1}{K_{S_p}+S}\right)\left(\frac{M_{ox}}{K_M+M_{ox}}\right)+q_{max_s}\left(\frac{x_s}{K_{S_s}+S}\right)\right)S\right]=0$$

(A6)

$$(1-p)\left[\frac{dx_p}{dt}-\left(\mu_{max,p}\left(\frac{S(t=0)}{K_{S_p}+S(t=0)}\right)\left(\frac{M_{ox}(t=0)}{K_M+M_{ox}(t=0)}\right)-K_{d_p}\right)x_p\right]$$
$$+p\left[\frac{dx_p}{dt}-\left(\mu_{max,p}\left(\frac{S}{K_{S_p}+S}\right)\left(\frac{M_{ox}}{K_M+M_{ox}}\right)-K_{d_p}\right)x_p\right]=0$$

(A7)

$$(1-p)\left[\frac{dx_S}{dt}-\left(\mu_{\max,s}\left(\frac{S(t=0)}{K_{S_s}+S(t=0)}\right)-K_{d_s}\right)x_S\right]$$
$$+p\left[\frac{dx_S}{dt}-\left(\mu_{\max,s}\left(\frac{S}{K_{S_s}+S}\right)-K_{d_s}\right)x_S\right]=0 \quad \text{(A8)}$$

$$(1-p)\left[\frac{dM_{OX}}{dt}+Y\left(q_{\max\,p}\left(\frac{S(t=0)}{K_{S_p}+S(t=0)}\right)\left(\frac{1}{K_M+M_{OX}(t=0)}\right)\right)M_{OX}-\frac{\gamma}{V_X p(t=0)}\frac{IMFC}{mF}\right]$$
$$+p\left[\frac{dM_{OX}}{dt}+Y\left(q_{\max\,p}\left(\frac{S}{K_{S_p}+S}\right)\left(\frac{1}{K_M+M_{OX}}\right)\right)M_{OX}-\frac{\gamma}{V_X p}\frac{IMFC}{mF}\right]=0$$

(A9)

The approximate solution of the equations (A6) to (A9) are

$$S=S_0+pS_1+p^2S_2+p^3S_3+.... \quad \text{(A10)}$$

$$x_p=x_{p_0}+px_{p_1}+p^2x_{p_2}+p^3x_{p_3}+... \quad \text{(A11)}$$

$$x_S=x_{S_0}+px_{S1}+p^2x_{S_2}+p^3x_{S_3}+... \quad \text{(A12)}$$

$$M_{ox}=M_{ox0}+pM_{ox1}+p^2M_{ox2}+p^3M_{ox3}+... \quad \text{(A13)}$$

Substituting Equations (A10) to (A13) into Equations (A6) to (A9) and comparing the coefficients of like powers $'p'$

$$p^0:\frac{dS0}{dt}+\left(q\max_p\left(\frac{1}{KS_p+Sin}\right)\left(\frac{Moxin}{KM+Moxin}\right)+q\max_s\left(\frac{xsin}{KS_s+Sin}\right)\right)S_O=0$$

(A14)

$$p^0:\frac{dx_{p_0}}{dt}-\left(\mu\max,p\left(\frac{Sin}{KS_p+Sin}\right)\left(\frac{Moxin}{KM+Moxin}\right)-Kd_p\right)xp_0=0 \quad \text{(A15)}$$

$$p^0:\frac{dx_S}{dt}-\left(\mu\max,s\left(\frac{Sin}{KS_s+Sin}\right)-Kd_s\right)xS_0=0 \quad \text{(A16)}$$

$$p^0:\frac{dMox_0}{dt}+Y\left(q\max_p\left(\frac{S}{KS_p+S}\right)\left(\frac{1}{KM+Mox}\right)\right)Mox-\frac{\gamma}{Vx p}\frac{IMFC}{mF}=0 \quad \text{(A17)}$$

The initial conditions are

$$S=S_{in},\ x_p=x_{pin},\ x_s=x_{\sin},\ M_{ox}=M_{oxin} \quad at \quad t=0 \quad \text{(A18)}$$

Solving Equations (A14) to (A17) with initial condition (A18), yields

$$S_0(t)=S_{in}e^{-t\left[\frac{q_{max_p}M_{oxin}x_{pin}}{(K_{S_p}+S_{in})(K_M+M_{oxin})}+\frac{q_{max_s}x_{Sin}}{K_{S_s}+S_{in}}\right]} \quad \text{(A19)}$$

$$x_{p_0}(t)=x_{pin}e^{t\left(\frac{\mu_{max_p}S_{in}M_{oxin}}{(K_{S_p}+S_{in})(K_M+M_{oxin})}-K_{d_p}\right)} \quad \text{(A20)}$$

$$x_{S_0}(t)=x_{Sin}e^{t\left(\frac{\mu_{max_S}S_{in}}{(K_{S_S}+S_{in})}-K_{d_S}\right)} \quad \text{(A21)}$$

$$M_{ox}(t)=M_{oxin}e^{-t(Yq_p)}+\frac{\gamma E_{OCV}}{Vx_{pin}mFYq_pR_{int}(\varepsilon+M_{red})}\left[M_{total}-M_{total}e^{-t(Yq_p)}-t\frac{YM_{oxin}e^{-t(Yq_p)}}{q_p}\right]$$

(A22)

The solution of the above equations as,

$$S(t)=S_0(t),\ x_p(t)=x_{p_0}(t),\ x_s(t)=x_{s_0}(t),\ M_{ox}(t)=M_{ox_0}(t)$$

$$S(t)=S_{in}e^{-t\left[\frac{q_{\max\,p}M_{oxin}x_{pin}}{(K_{S_p}+S_{in})(K_M+M_{oxin})}+\frac{q_{\max\,s}x_{Sin}}{K_{S_s}+S_{in}}\right]} \quad \text{(A23)}$$

$$x_p(t)=x_{pin}e^{t\left(\frac{\mu_{\max\,p}S_{in}M_{oxin}}{(K_{S_P}+S_{in})(K_M+M_{oxin})}-K_{d_p}\right)} \quad \text{(A24)}$$

$$x_S(t)=x_{Sin}e^{t\left(\frac{\mu_{\max\,S}S_{in}}{(K_{S_S}+S_{in})}-K_{d_S}\right)} \quad \text{(A25)}$$

$$M_{ox}(t)=M_{oxin}e^{-t(Yq_p)}+\frac{\gamma E_{OCV}}{Vx_{pin}mFYq_pR_{int}(\varepsilon+M_{red})}\left[M_{total}-M_{total}e^{-t(Yq_p)}-t\frac{YM_{oxin}e^{-t(Yq_p)}}{q_p}\right]$$

(A26)

REFERENCES

[1] V.M. Ortiz-Martnez , M.J. Salar-Garca , A.P. de los Ros, F.J. HernndezFernndez, J.A. Egea, L.J. Lozano. Developments in microbial fuel cell modeling, Chem. Eng J, 271,pp.50-60, 2015.

[2] D. Recio-Garrido, M. Perrier, B. Tartakovsky, Modeling, optimization and control of bioelectrochemical systems, Chem. Eng J, 289,pp.180-90, 2016.

[3] C. Xia, D. Zhang, W. Pedrycz, Y. Zhu, Y. Guo, Models for microbial fuel cells: a critical review, J Power Sources, 373, pp. 119-31, 2018.

[4] R.P. Pinto, B. Srinivasan, M.F. Manuel, B. Tartakovsky, A two population bio-electrochemical model of a microbial fuel cell, Bioresour Technol, 14, pp. 5256-65, 2010.

[5] M. Esfandyari, M.A. Fanaei, R. Gheshlaghi, M. AkhavanMahdavi, Dynamic modeling of a continuous twochamber microbial fuel cell with pure culture of shewanella, Int J Hydrogen Energy, 33, pp.21198-202, 2017.

[6] A.G Capodaglio, E. Ranieri, V. Torretta, Process enhancement for maximization of methane production in codigestion biogas plants, Manag. Environ. Qual. Int. J, 27, pp.289–298, 2016.

[7] A.G. Capodaglio, A. Callegari, Feedstock and process influence on biodiesel produced from waste sewage sludge, J. Environ. Manag, 2017.

[8] Siddharth Gadkari, Mobolaji Shemfe, Jhuma Sadhukhan, Microbial fuel cells: A fast converging dynamic model for assessing system performance based on bioanode kinetics, International Journal of hydrogen energy, 44, pp.15377-15386, 2019.

[9] G. Andrea, Capodaglio, Daniele Cecconet and Daniele Molognoni, An Integrated Mathematical Model of Microbial Fuel Cell Processes, Bioelectrochemical and Microbiologic Aspects, 2017.

[10] J.H He, Homotopy perturbation technique, Compt. Method. Appl. Mech. Engg, 178, pp.257-262, 1999.

[11] A.A Hemeda, Application of homotopy perturbation method to nonlinear wave equations, App. Math. Sci., 6, pp. 4787 – 4800, 2012.

[12] S. Ganesan, S. Anitha, A. Subbiah, L. Rajendran, Homotopy perturbation method for solving systems of nonlinear coupled equations, J. Memb. Biol, 246, pp. 435-442, 2013.

[13] A. Meena, L. Rajendran, Mathematical modeling of amperometric and potetiometric biosensors and system of nonlinear equations-Homotopy perturbation approach, J. Electroanal. Chem, 644, pp. 50-59, 2010.